JOURNAL OF BACTERIOLOGY, May 1993, p. 3174–3181
0021-9193/93/103174-08$02.00/0

Vol. 175, No. 10

Volume Growth of Daughter and Parent Cells during the Cell Cycle of *Saccharomyces cerevisiae* a/α as Determined by Image Cytometry

CONRAD L. WOLDRINGH,* PETER G. HULS, AND NORBERT O. E. VISCHER

Department of Molecular Cell Biology, Section of Molecular Cytology, University of Amsterdam, Plantage Muidergracht 14, 1018 TV Amsterdam, The Netherlands

Received 5 November 1992/Accepted 14 March 1993

The pattern of volume growth of *Saccharomyces cerevisiae* a/α was determined by image cytometry for daughter cells and consecutive cycles of parent cells. An image analysis program was specially developed to measure separately the volume of bud and mother cell parts and to quantify the number of bud scars on each parent cell. All volumetric data and cell attributes (budding state, number of scars) were stored in such a way that separate volume distributions of cells or cell parts with any combination of properties—for instance, buds present on mothers with two scars or cells without scars (i.e., daughter cells) and without buds—could be obtained. By a new method called intersection analysis, the average volumes of daughter and parent cells at birth and at division could be determined for a steady-state population. These volumes compared well with those directly measured from cells synchronized by centrifugal elutriation. During synchronous growth of daughter cells, the pattern of volume increase appeared to be largely exponential. However, after bud emergence, larger volumes than those predicted by a continuous exponential increase were obtained, which confirms the reported decrease in buoyant density. The cycle times calculated from the steady-state population by applying the age distribution equation deviated from those directly obtained from the synchronized culture, probably because of inadequate scoring of bud scars. Therefore, for the construction of a volume-time diagram, we used volume measurements obtained from the steady-state population and cycle times obtained from the synchronized population. The diagram shows that after bud emergence, mother cell parts continue to grow at a smaller rate, increasing about 10% in volume during the budding period. Second-generation daughter cells, i.e., cells born from parents left with two scars, were significantly smaller than first-generation daughter cells. Second- and third-generation parent cells showed a decreased volume growth rate and a shorter budding period than that of daughter cells.

Because of its polarized growth and asymmetric division, a population of the budding yeast *Saccharomyces cerevisiae* consists of two subpopulations: daughter cells without scars and parent cells which bear one or more scars and which are usually larger (8). The degree of size asymmetry at division is dependent on the growth rate, with more slowly growing cells dividing more asymmetrically (12).

After a yeast cell has divided, the parent cell, with one newly acquired bud scar, is in a state in which almost all of its growth potential has been directed to a single site, the bud neck, now replaced by the scar structure. It must determine a new position for its bud site to continue polarized growth. The daughter cell, on the other hand, is growing in an apolar way and continues its diffuse expansion until it also switches to bud growth. The occurrence of such a switch from diffuse, apolar growth to polarized growth at the bud site can be expected to cause a discontinuity or rate change in the overall growth pattern of the daughter cell, for instance, with respect to volume increase.

In most bacteria and eukaryotic cells, however, cell volume and mass increase in a smooth, exponential process (3). Nevertheless, changes in rate of protein synthesis have been suggested to occur during the cell cycle of *Schizosaccharomyces pombe* (14), although such findings have been criticized (3). Biochemical studies of *S. cerevisiae* have suggested both the presence (4, 18) and absence (5, 15) of periodic changes in enzyme activity during the cell cycle. In view of the complexity of yeast populations, such suggestions are difficult to evaluate without precise information on the volume growth pattern of individual yeast cells, both during the cycle of the daughter cell and during that of parent cells.

Most information on the growth pattern of daughter and parent cells in yeast populations has been obtained by time-lapse studies of relatively small numbers of cells (8, 20). In addition, quantitative data on the mean sizes of daughter and parent cells at birth and division are scarce. Most studies have concentrated on the variation in average cell volume or cycle periods as a function of growth rate (10, 12, 16). Lord and Wheals (13) and Wheals (20) measured the mean size of *S. cerevisiae* cells at birth and at bud emergence by using time-lapse microscopy but could make no distinction between daughter cells and parent cells of different genealogies. This also holds true for flow cytometric studies. In their analysis of DNA and protein distributions made with a flow cytometer, Vanoni et al. (19) could only derive the growth mode of cells for the different subpopulations by making a number of assumptions, including (i) exponential protein increase, (ii) constancy of the budded period for both daughter and parent cells of different genealogical ages, (iii) a certain coefficient of variation (CV) of the size of daughter and parent cells at division, and (iv) a size increment between consecutive cycles of parent cells.

In contrast to flow cytometry applied in previous growth studies of the budding yeast (16, 19), image cytometry

* Corresponding author. Electronic mail address: a430coli@diamond.sara.nl.

combined with bud scar analysis can provide direct information on the volume growth of either daughter or parent cells. In the present study, we applied a two-dimensional image analysis and contour rotation program developed for separate measurement of the volumes of buds and mother cells (9). By using the volume measurements of cells from a steady-state population and the cycle times of synchronized cells, we have constructed a volume-time diagram which demonstrates the volume growth of daughter cells and consecutive cycles of parent cells, both for the whole cell and for the mother cell parts. The results indicate an exponential volume increase with a slight acceleration after bud emergence.

MATERIALS AND METHODS

Organism and medium. The diploid yeast strain *S. cerevisiae* X2180 (a/α *CUP1/CUP1 gal2/gal2 mal/mal mel/mel SUC2/SUC2*), was constructed with the use of haploid strains obtained from the Yeast Genetic Stock Center (Berkeley, Calif.) and has been used throughout. Cells were grown in a defined medium consisting of 0.7% yeast nitrogen base without amino acids and ammonium sulfate (YNB 0335-15-9; Difco Laboratories, Detroit, Mich.) supplemented with 2% glucose, 0.5% ammonium sulfate, and 4.7 g of NaCl per liter to increase the osmolality of the medium to 300 mosM. The pH of the medium was 5.4. Cell suspensions in 250-ml or 3-liter Erlenmeyer flasks were shaken in a water bath at 30°C.

Growth measurement and criterium for steady-state growth. Growth was monitored by measuring the optical density of the culture at 450 nm (OD_{450}). The number of cells was determined with an electronic particle counter constructed in our laboratory and with a 70-μm orifice tube from Coulter Electronics Ltd. (Luton, England). At all times, the cell concentration was kept below 2.5×10^6 cells per ml by periodic dilution of the culture. Constancy of average cell mass, expressed as OD per cell, was obtained after about 20 generations of unperturbed growth at a mass doubling time of 118 to 125 min and was considered to represent the steady state of growth.

Synchronization by centrifugal elutriation. Four liters of cells was centrifuged at 4°C and resuspended in 10 ml of culture medium. The cells were kept at 4°C in all subsequent steps. The elutriation chamber of a 5-ml (Beckman JE-6B elutriator rotor; Beckman Instruments, Inc., Palo Alto, Calif.) was loaded with about 10^{10} cells and equilibrated for 30 min. Small cells were collected at flow rates of between 12 and 14 ml/min and at 2,750 rpm. About 150 ml of small cells collected from the rotor was centrifuged at 4°C and resuspended in 300 ml of growth medium to start synchronous growth. In a separate experiment, the whole culture was collected after a 30-min equilibration in the rotor. Such control cultures generally grew with a 10-min-longer mass doubling time than the original batch culture. The synchronization indices calculated with the formula of Blumenthal and Zahler (2) and using the cycle time of daughter cells as the generation time (e.g., t_d = 150 min) were about 0.55. Further details of the procedure have been described previously (7, 18).

Bud scar analysis. Cells were fixed by directly adding samples to an equal volume of cold ethanol (−20°C). They were stored at 4°C until analysis. For fluorescence microscopy, cells were centrifuged and resuspended in 30 μg of Calcofluor (fluorescent brightener; Sigma) per ml in 0.9% NaCl, incubated at room temperature for 1 h, and washed three times with 0.9% NaCl. Hoechst 33342 was used at a concentration of 1 μg/ml in distilled water for scoring nuclear morphology. Cells were directly prepared on an object slide without immobilization and observed with a Zeiss Universal fluorescence microscope, equipped with a Neofluar 100×/1.3 phase-contrast lens. The preparation was excited with light below 380 nm, and the emitted light was detected above 420 nm.

Image cytometric measurement of cell volume. Images of cells stained with Calcofluor as described above were captured when buds and mother cells were lying in focus. We used a Grundig CCD video camera type FA 85 I, a Macintosh IIci computer, and a Data Translation DT2250 framegrabber. Out of the live picture, each cell of interest was measured with a customized version of the image analysis program Image 1.43 (Rasband; National Institutes of Health [9]) and then copied together with an appropriate amount of background into a collect file for further reference. Numerical data were stored as text files, from which any desired combination of subpopulations (number of scars, buds, etc.) could be extracted and processed via a spreadsheet program. Images were calibrated with a micrometer slide.

RESULTS

Characterization of a steady-state population. To establish the volume growth pattern of the individual yeast cell, the average volumes of daughter and parent cells at birth and at division must be known. To determine these volumes, we first measured buds and mother cells in a steady-state population of *S. cerevisiae* growing with a doubling time (T_d) of 118 min. The volume distribution (V) obtained by image cytometry shows the expected large variation in size, ranging from a minimum of 14 μm^3 to a maximum of 125 μm^3 (Fig. 1). The shape of the distribution is slightly bimodal because of the summation of a skewed daughter cell distribution (Fig. 1B) and an almost symmetrical distribution of parent cells (Fig. 1C). The latter is again a summation of the subdistributions of parents with one, two, and more scars (separate distributions not shown). From the fraction of daughter cells [F(D)] and parent cells [F(P)] in the population, estimated by bud scar analysis, their average generation times can be calculated by applying the formula of the age distribution (12). The results are presented in Table 1, together with the duration of the budding period (t_b) derived from the fraction of budded cells [F(B)], without making a distinction between daughter and parent cells. According to this calculation, no unbudded parent cells would be present in the population, because t_b (87.5 min) is found to be larger than the generation time for parent cells (t_p; 86 min). However, according to the bud scar analysis, the fraction of unbudded parent cells [F(PU)] in the total population was 7.9% and, on average, the F(PU) was 25% in the subpopulations of parents of different genealogies (Table 1). Taking account of the F(PU) and fraction of unbudded daughter cells [F(DU)] suggests that the budding periods may be different, i.e., 104 and 73 min for daughter and parent cells, respectively, and that the duration of the unbudded period for parent cells is 13 min ($t_p - t_{bp}$ in Table 1).

Volume of newborn cells. To obtain the mean volume of newborn daughter cells, we assumed that their distribution is represented by the intersection between the following two subdistributions: (i) the V of the buds on mother cells (open distribution in Fig. 2) and (ii) the V of daughter cells without buds (hatched area in Fig. 2). The right-hand side of the first

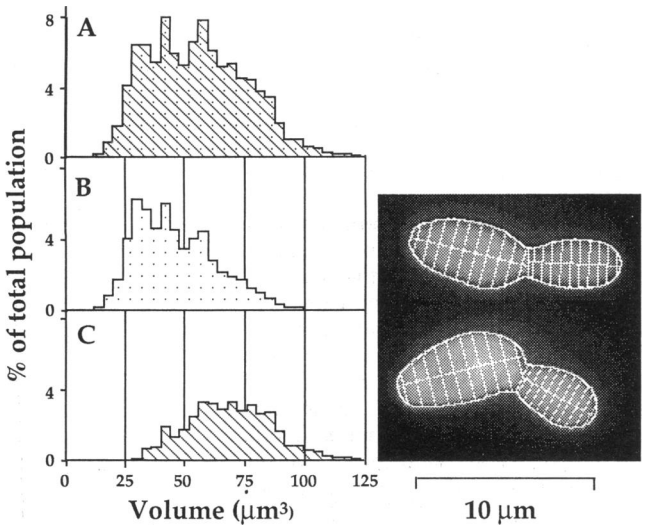

FIG. 1. Cell Vs of *S. cerevisiae* as determined by image cytometry of cells stained with Calcofluor. The doubling time of the steady-state population was 118 min. The distribution of the total population (A) has an average volume of 56 μm^3 with a CV of 36%. Because the measuring system also allows for the detection of bud scars, subdistributions of daughter cells (i.e., cells without scars [B]) and parent cells (i.e., cells with one or more scars [C]) are given. The distribution of daughter cells has an average of 47 μm^3 (CV, 36%) and that of parent cells has an average of 69 μm^3 (CV, 25%). The two cells (right panel) are representative examples taken from the collect file (see Materials and Methods). Cell contours and sections were determined with the image analysis program as described in reference 9.

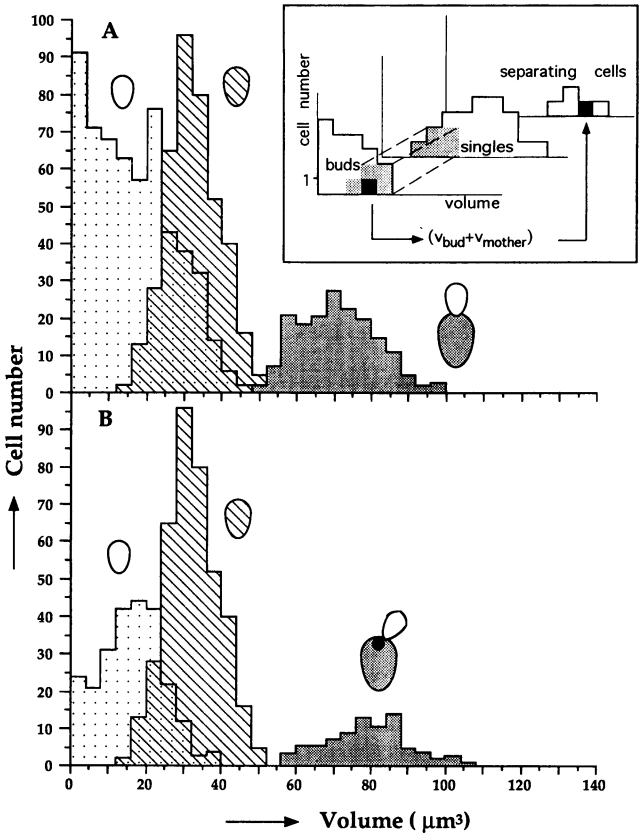

FIG. 2. Determination of the V of newborn cells derived from parent cells without scars (A [V_{D1}]) and from parent cells with one scar (B [V_{D2}]). In this so-called intersection analysis (see text), buds (dotted open distribution) are sorted out from the distribution of parent cells with a volume and frequency that correspond to the area overlapping the distribution of single cells without buds or scars (hatched distribution). By adding the corresponding volume of the mother cell part to the selected bud volumes, the V_{P1} and V_{P2} at cell separation are obtained (shaded distribution). The results of the analysis are summarized in Table 2. (Inset) Each bud in the shaded intersection area (where buds and single cells overlap) is combined with its mother cell to build the histogram of separating cells.

distribution contains the largest buds which have not yet separated from the mother cell by division. The left-hand side of the second distribution contains the smallest cells which separated from dividing mothers. The overlapping area of these two distributions is assumed to reflect the size range of newborn daughter cells. If we take, for the first distribution, the buds on mother cells without scars, the intersection represents the V of newborn, first-generation daughter cells ([V_{D1}] Fig. 2A): the average of this distribution was found to be $V_{D1} = 28.5\ \mu m^3$. If we take, for the first distribution, the buds on parents with one scar (Fig. 2B), we obtain the distribution of newborn, second-generation daughters (V_{D2}). Surprisingly, the average of this distribution, $V_{D2} = 24.4\ \mu m^3$, is smaller than that of V_{D1}. As can be seen in Fig. 2B, the smallest Vs of buds on parents with one scar are underrepresented. The reason is that in 90% of the cells, the second bud emerges sideways (Fig. 1) next to the first scar and, when still small, usually lies out of focus when the parent cell is imaged in focus. As a result, these smallest buds are not detected by the contour analysis program. This phenomenon does not hold for the larger buds and therefore does not affect the intersection analysis. The results of the calculations are summarized in Table 2 (column 2) and suggest that the volumes of second- and higher-generation daughters remain smaller than those of the first-generation daughters. However, considering the CVs of 12 to 15% (Table 2), we can only conclude that the higher-generation daughters are at least not larger than the first-generation daughters (see Discussion).

TABLE 1. Sizes of subpopulations and cell cycle times[a] of daughter and parent cells as calculated from a steady-state population of 6,243 cells

Cell fraction	% of total population average (SD)[b]	Calculated cycle period average (SD)[b]
F(D)	60.3 (1.8)	t_d, 157.5 (7)
F(P)	39.7 (1.7)	t_p, 86 (4.5)
F(B)	66.9 (4.0)	t_b, 87.5 (3.9)
F(DU)	25.1	t_{bd}, 104[c]
F(PU)	7.9	t_{bp}, 73[c]

[a] Cycle times were calculated by using the equations derived by Lord and Wheals (12) and an overall T_d of 118 min.

[b] SD, standard deviation, was obtained from four independent microscopic preparations measured by two observers.

[c] Calculated by using the F(DU) and F(PU). The F(DU) represented about 50% of the F(D). This gives a duration of 54 min for the unbudded period. The F(PU)s of the different genealogies represent 25% of the respective fractions, leading to a duration of 13 min ($t_p - t_{bp}$) for the unbudded period. Subtracting these periods from the cycle times gives the respective t_{bd} and t_{bp}. The formula used for calculating the unbudded period for daughters is derived by integrating the expression of the age distribution (equation 3 in reference 12) between appropriate limits: $t_{bd} = t_d - \{T_d \cdot \ln[1 - F(DU)]\}/\ln 2$.

Volume of cells at division. To obtain the V of cells at

TABLE 2. Average volumes at birth, division, and bud emergence for different generations as obtained by intersection analysis of the steady-state population[a]

Daughter cells				Parent cells				No. of cells scored[e]
Generation	Vol. at:			Generation	Vol. at:			
	Birth[b]	Bud emergence[c]	Division		Birth[d]	Bud emergence[c]	Division	
1	28.5 (15)[f]	38.5 (16)	70.7					958
2	24.4 (14)			1	42.2	46.8 (16)	79.0	302
3	24.2 (13)			2	54.6	56.1 (15)	82.4	165
4	22.3 (15)			3	58.2	63.9 (16)	88.9	82
≥5	22.2 (12)			≥4	66.6	71.4	97.5	77

[a] Results are given for the same population as shown in Fig. 1 and 2 and Table 1.
[b] Average volume represented by the intersection of the distribution of buds on mother cells with that of daughter cells without buds (Fig. 2).
[c] Volume of mother cells containing buds smaller than 4 μm³.
[d] Obtained as $V_{CS} - V_D$. Note that V_{P1} (42.2) + V_{D1} (28.5) = V_{CS} (70.7) and that V_{P2} (54.6) + V_{D2} (24.4) = V_{CS1} (79.0).
[e] First distribution used in the intersection analysis (Fig. 2).
[f] Values in parentheses are CVs.

division or cell separation (V_{CS}), the volume of every individual bud found within the intersection (Fig. 2) is added to the volume of its mother cell part (Table 2, columns 4 and 8). Subtracting the volume of the newborn daughter cell (V_D) from that of the dividing cell (V_{CS}) gives the volume of the newborn parent cell of the next generation ([V_P] Table 2, column 6). These results show that an average newborn daughter cell increases in volume by a factor of 3 before division, from about 24 to 70.7 μm³. The V_P increases after the first cycle by some 30% and increases during consecutive cycles by about 10%, to a maximum volume of 74 μm³. At division, a maximum average value of 97.5 μm³ was obtained for parent cells of the fourth generation (Table 2, column 8).

V_{BE}. To obtain the volume of cells at bud emergence (V_{BE}), the volume of every bud smaller than 4 μm³ (Fig. 2) was added to the volume of its mother cell part. Just as with the intersection analysis, this procedure could be repeated with the buds on mother cells of different genealogies. The different distributions thus obtained were considered to represent the V_{BE}. In Table 2 (columns 3 and 7) it can be seen how this volume increases from 38.5 to 71.4 μm³ and how the distributions show a CV of 16%. This variation is rather smaller than the 22 to 25% found previously in time-lapse experiments (13, 20). Comparison of the volumes of parent cells in columns 6 and 7 in Table 2 shows that parents increase significantly in volume between birth and bud emergence.

Mode of volume growth of synchronized cells. To determine the pattern of volume growth between birth and division, we monitored the growth of a synchronous population obtained by centrifugal elutriation. Two synchronous cultures were started with fractions of small cells selected from the steady-state population described above (Table 1 and Fig. 1 and 2) at flow rates of 13 and 14 ml/min, respectively. Because the latter fraction already contained some budded cells (5%) and cells with scars (3%), the synchronous culture of the fraction eluted with a flow rate of 13 ml/min was analyzed further. It contained 0.4% budded cells and 0.3% cells with a scar. As can be seen in Fig. 3A, cell mass as indicated by the OD_{450} increased exponentially. However, the rate of increase corresponds to a doubling of the initial mass in 170 min. By contrast, the doubling in cell number, as indicated by the time 50% of the cells had divided, occurred at 150 min. This is somewhat shorter than the doubling time calculated for daughter cells from the steady-state population (t_d = 157.5

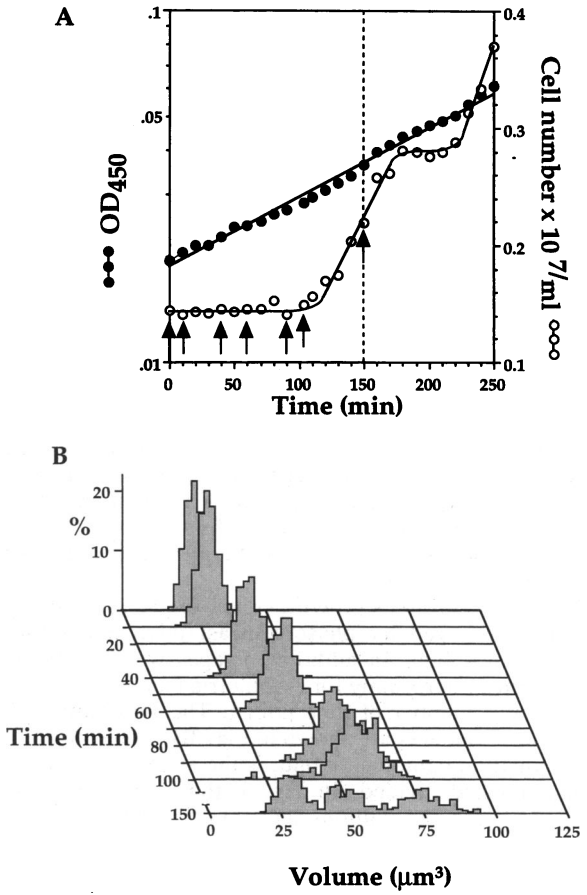

FIG. 3. (A) Increase in OD and cell number during synchronous growth of small cells selected from the steady-state population shown in Fig. 1 at a flow rate of 13 ml/min. Arrows indicate samples used for image cytometric measurement of cell volume. At about 150 min, 50% of the selected cells have divided. (B) *V*s of cells stained with Calcofluor. The average values for the first six consecutive samples are 25.9, 27.6, 40.6, 52.2, 56.9, and 74.3 μm³. The CVs of these distributions were 15% for the first sample and 12 to 13% for the others (not considering cells which have divided). At 60 min, 50% of the cells contained a bud. At 150 min, cells are in the process of division, giving rise to three peaks: first-generation daughter cells, parent cells with one scar, and dividing cells. The small cells at 0 min, selected with the elutriator, represent a mixture of first- to higher-generation daughter cells.

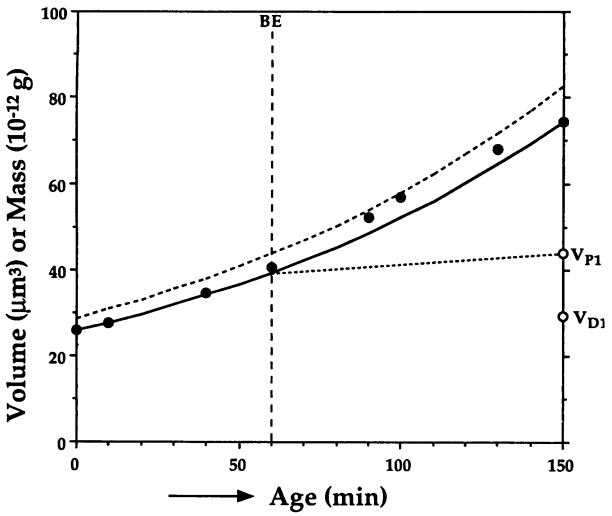

FIG. 4. Mode of volume increase for mixed-generation daughter cells selected with the elutriator. Average cell volumes, calculated from the distributions shown in Fig. 3B, are plotted on a linear scale as a function of time of synchronous growth. The solid line represents an exponential volume increase calculated for a daughter cell of 25.9 μm^3 which reaches a volume at division of 74.3 μm^3 in 150 min (see Fig. 3). The dashed exponential line represents the mass increase, assuming a constant density of 1.111 g/ml. The open symbols at 150 min represent the V_{D1} (29.2 μm^3) and V_{P1} (44.2 μm^3) obtained by intersection analysis (Fig. 2) of the sample at 150 min. The vertical dashed line (BE) at 60 min indicates the time of bud emergence.

min; Table 1). The average volume of the cells in this starting fraction (mixed-generation daughter cells) was 25.9 μm^3 (Fig. 3B), i.e., a value between that for first- and second-generation daughter cells, as determined from the steady-state culture by the intersection analysis (see above and Table 2). The shorter doubling time of 150 min can thus not be explained by assuming that the cells selected at 13 ml/min were too large and too old and is therefore probably correct (see below and Fig. 6).

During synchronous growth, cells were sampled every 10 min and observed by phase-contrast microscopy for the presence of a bud. In addition, images were captured by fluorescence microscopy for cytometric measurement of cell volume at a number of time points. The Vs obtained from these measurements are shown in Fig. 3B. At 60 min, 50% of the population contained a bud, while at 150 min half of the population had divided. In Fig. 4, the average values obtained from the distributions shown in Fig. 3B are plotted on a linear scale as a function of time during synchronous growth. The eight points show that during the first part of the daughter cell cycle, volume increases exponentially. After bud emergence at 60 min, however, the measured volume values are slightly higher than predicted by an exponential increase. If cell mass would increase exponentially, as indicated by the dashed line in Fig. 4, cell density would decrease after bud emergence. A decrease in buoyant density (0.7%) has indeed been observed by Baldwin and Kubitschek (1) and was confirmed for our strain and synchronization procedure (results not shown). The increase in OD shown in Fig. 3A does not at all follow the dashed line given in Fig. 4. In our view, OD measurements of budding cells therefore have to be interpreted with great care.

Applying the intersection analysis to the cells at 150 min (see open symbols at 150 min in Fig. 4), we obtained a V_{D1} of 29.2 μm^3, which is in good agreement with the 28.5 μm^3 found for the steady-state population (Table 2). The V_{BE} (BE in Fig. 4) was 40 μm^3, which also compares well with the 38.5 μm^3 for steady-state daughter cells in their first generation (Table 2). It can be seen from the volume data in Fig. 4 that, after bud emergence, the mother cell part continued to grow about 10% in volume to a V_{P1} of 44.2 μm^3.

Determination of cycle times from synchronized cells. In a second synchronization experiment, cells were again collected at a flow rate of 13 ml/min from a steady-state population with a T_d of 120 min. In this experiment, samples were taken for fluorescence microscopy to score the percentage of budded cells in subpopulations of daughter cells (Fig. 5A) and of parents with one, two, and three scars (Fig. 5B). From these graphs, the cycle time (t_d) of first-generation daughter cells (i.e., daughter cells divided from daughter cells) can be determined from the first time to the second time that 50% of the daughters show a bud (Fig. 5A). The second peak of budded daughter cells in Fig. 5A is lower than the first because, after about 200 min, (unbudded) daughter cells are produced by cells with one scar (first peak in Fig. 5B). The cycle time of first-generation daughters is slightly shorter (t_d = 147 min) than the 150 min obtained from the selected cells (mixed-generation daughter cells) in the experiment shown by Fig. 3 and 4.

From the time that 50% of the daughter cells have divided (vertical line in Fig. 5) to the time that 50% of budded cells with one scar have divided (Fig. 5B), the cycle time for parents with one scar (t_{p1}) can be estimated. By a similar reasoning, the cycle times for consecutive generations of parents (t_{p2}, t_{p3}) are obtained (Table 3). The plots suggest that these cycle times are of similar durations, because the budding periods derived from the time when the cells of a subpopulation have increased to 50% to the time when they have decreased to 50% by division. However, in the samples, unbudded parents were clearly present. Apparently, the period of 10 min between the samples in Fig. 5 is, relative to an unbudded period of 13 min (Table 1), too long to permit an accurate estimate of budding periods.

Construction of a volume growth pattern based on data from steady-state and synchronous cultures. Combining the volume data derived from the steady-state population (Table 2) with the cycle time data obtained with the synchronous cells (Fig. 5 and Table 3), a volume-time diagram can be constructed as shown in Fig. 6. The diagram shows on an exponential volume scale (Fig. 4) the rates of volume growth for the different subpopulations. The V_{BE}s (indicated by arrows in Fig. 6) are also obtained from Table 2. However, the respective budding periods were not taken from Table 3, because they suggest the absence of unbudded periods. Instead, we found it more realistic to place the points according to the duration of the unbudded periods of 54 min for daughter cells and 13 min for parent cells, as calculated from the steady-state population (Table 1). For the first generations (D1 and P1) the growth rates are similar, whereas later generations (P2 and P3) seem to grow at a slightly slower rate in shorter cycle times. The results further show that first-generation daughter cells are larger than second- and higher-generation daughter cells. Whether the latter subpopulation shows a longer cycle time, as assumed in Fig. 6, remains to be established by independent methods (see Discussion).

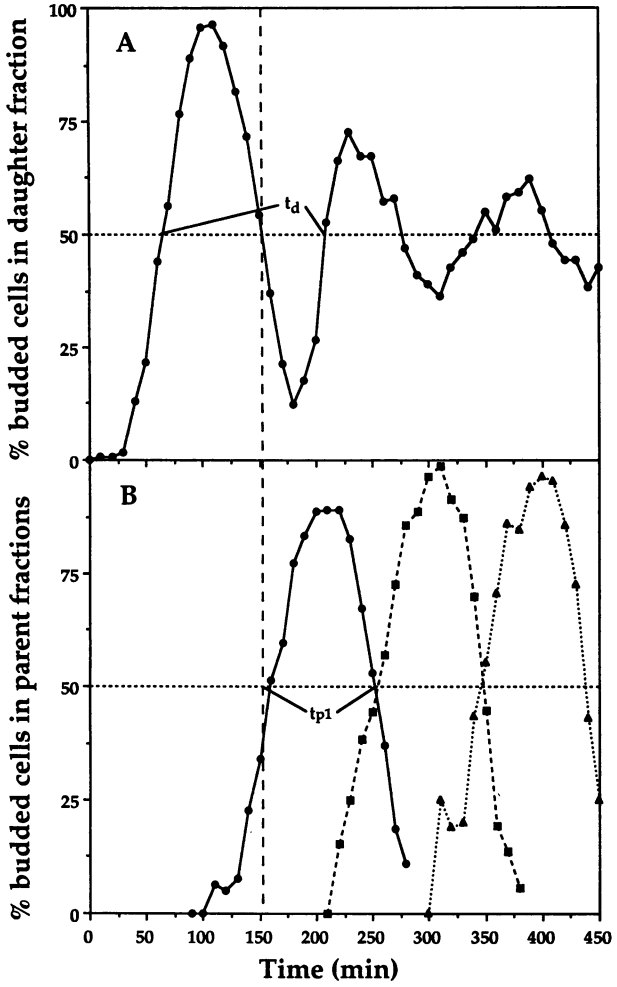

FIG. 5. Changes in budding state during synchronous growth of small cells selected from a steady-state population growing with a mass doubling time of 120 min. Dashed horizontal lines indicate values where 50% of the cells in a time sample show a bud. (A) Daughter cells without scars. At 63 min, 50% of the cells have acquired a bud. At 151 min (dashed vertical line), 50% of the cells have lost their bud through division, suggesting a t_b of 88 min for daughter cells. At 210 min, the daughter cells have again acquired a bud, resulting in a generation time (t_d) of 147 min (Table 3). (B) Parent cells with one (●), two (■), or three (▲) scars. Budding periods and generation times can be derived as for daughter cells (Table 3).

TABLE 3. Duration of cell cycle periods of daughter and parent cells of different genealogies as directly determined from the synchronized population in Fig. 5

Subpopulation	Cell cycle period[a]	
	Cycle time (min)	Budding period (min)
Daughter cells	t_{d1}, 147	t_{bd1}, 88
Parent cells with:		
1 scar	t_{p1}, 103	t_{bp1}, 91
2 scars	t_{p2}, 93	t_{bp2}, 92
3 scars	t_{p3}, 91	t_{bp3}, 91

[a] Compare with cycle periods calculated from the steady-state population in Table 1.

DISCUSSION

The image cytometric measuring system described previously (9) has been applied here to *S. cerevisiae* cells from both steady-state and synchronous populations. The volume measurements show how the daughter cells in the population largely follow an exponential volume growth pattern (Fig. 4). After bud emergence, however, a deviation occurs which may be related to the decrease in buoyant density found in the later part of the cell cycle (1). Such a density variation (0.7%) has not been found in other organisms, including *S. pombe* (11). For a cell consisting of about 30% dry mass, a density decrease of 0.7% implies that the concentration of solid compounds has to decrease by 20%, assuming that the density of dry solids remains constant. The decrease may be related to the growth of the bud, which, because of a more elastic cell wall, allows temporally a more than exponential volume increase during most of the budding period. The volume measurements of synchronized cells (Fig. 4) give no indication for an abrupt change in volume growth rate. Although a gradual response could be ascribed to the fact that average values have been measured, it is our impression

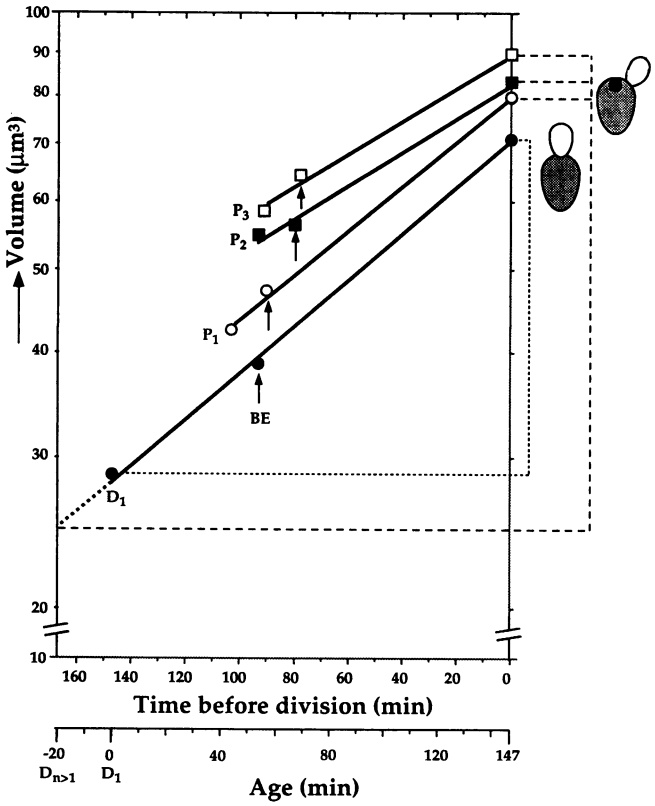

FIG. 6. Volume growth during the cell cycle of first-generation daughters (D_1) and consecutive generations of parents (P1 to P3). The values for cell volume are those calculated from the steady-state population (Table 2). The cycle times are those obtained for the synchronous population (Table 3). The V_{BE}s obtained in Table 2 and indicated by arrows are placed on the time axis by taking into account the durations of the unbudded periods (Table 1): 54 min for daughter cells and 13 min for parent cells. Solid lines are regression lines through the three points. Note the exponential scale for volume. Dashed lines indicate the volumes of first- and higher-generation daughter cells.

that the emergence and growth of the bud is not an abrupt process and does not represent a discontinuity in the rate of volume growth or protein synthesis as predicted by a linear growth model (14; see also discussions in reference 3) and some biochemical studies (4, 18).

By application of a novel method, called intersection analysis, the average volumes of newborn and of dividing daughter and parent cells could be calculated (Table 2). The method relies on the assumption that the size and frequency of those buds on mother cells which overlap the distribution of single cells (see intersection, Fig. 2) represent the distribution of newborn daughter cells and that this same distribution of buds, with their mother cell parts added, represents the V of dividing cells. The volumes (Table 2) compared well with those of synchronized cells (Fig. 3 and 4) and also agree with published values for a diploid strain (17).

With respect to cell cycle periods, discrepancies between the cycle times calculated for the steady-state population (e.g., t_d = 157.5 and t_p = 86 min; Table 1) and those directly obtained for synchronous populations (e.g., t_d = 147 and t_p = 103 to 91 min; Table 3) were found. These discrepancies can be ascribed to a shortage of parent cells (especially of higher genealogies) scored during bud scar analysis of the steady-state population. Such a shortage has also been remarked upon by Lord and Wheals (12), who therefore used a different way of calculating the cycle times, based on the scoring of both buds and bud scars. However, their formula (see equation 8 in reference 12) cannot abolish an inadequate scoring of bud scars.

Another consequence of scoring too few parent cells in the steady-state population is the outcome of the budding period. When assuming that the budding period is equal for daughter and parent cells, the budding period appears to be longer than the corresponding parent cell cycle time (see Table 1). When calculating the budding periods from the fractions of unbudded cells (8), the budding period for daughter cells (t_{bd} = 104 min) is much longer than that for parents (t_{bp} = 73; Table 1). The relatively rough estimates of the budding periods from synchronized populations (Fig. 4 and 5) show that the budding periods are all very similar, ranging from 88 to 92 min (Table 3). Nevertheless, in all subpopulations of parent cells, both in the steady-state population (Table 1) and in synchronized cells (Fig. 5), a significant fraction of unbudded cells occurred. Because of this fact and also because the volume of parent cells at bud emergence is larger than at birth (Table 2), we consider the existence of an unbudded period as realistic. Therefore, we decided to use the values of unbudded periods calculated in Table 1 for the construction of the volume-time diagram shown in Fig. 6. This implies that the budding period for daughter cells is 93 min and that for parents is 90 to 78 min, despite previous studies (12, 19) and our own results with synchronized cells (Fig. 5).

The present calculations of the volume of newborn daughter cells by the intersection analysis indicate that first-generation daughter cells are larger than second- or higher-generation daughter cells. Whether the first-generation daughter cells also have a shorter cycle time than the higher-generation daughter cells, as suggested in Fig. 6, is difficult to establish. With the centrifugal elutriator, only mixed-generation daughter cells can be selected (Fig. 3). However, by reloading the elutriator chamber with daughter cells (collected at 4°C), by allowing them to grow and divide at 30°C, and by continuously eluting the small daughter cells, it is possible to collect consecutive generations of daughter cells. Preliminary experiments confirmed that the daughter cells of the second and subsequent generations are indeed smaller than those of the first generation but did not indicate significant changes in cycle times (to be published elsewhere).

Our results contrast with the model proposed by Vanoni et al. (19), in which older parent cells produce larger daughter cells with shorter cycle times. Their model necessarily generates a large variability in cell sizes which seems to contradict the relatively narrow distribution of daughter cells that were obtained from the intersection analysis (Table 2) and could be selected with the elutriator (see Fig. 3B). Both methods generated a distribution of daughter cells with a CV not larger than 15%.

Their proposal that each new generation of parent cells requires an increased protein level for bud emergence is in accordance with our finding of an increased V_{BE} (Fig. 6), which was also found previously in bud scar analyses of steady-state populations (10). However, an increased cell volume does not imply an increased protein content if the volume of the vacuole becomes larger in older parent cells. We are presently measuring the average vacuolar volumes in the various subpopulations of daughter and parent cells by applying our image cytometric system to living cells stained with fluorescein isothiocyanate (6).

ACKNOWLEDGMENTS

We thank N. Nanninga for suggestions and critical comments on the manuscript and A. E. Wheals, J. M. Mitchison, K. van Dam, L. J. W. M. Oehlen, and N. B. Grover for stimulating discussions.

REFERENCES

1. **Baldwin, W. W., and H. E. Kubitschek.** 1984. Buoyant density variation during the cell cycle of *Saccharomyces cerevisiae*. J. Bacteriol. **158**:701–704.
2. **Blumenthal, L., and S. A. Zahler.** 1962. Index for measurement of synchronization of cell populations. Science **135**:724–726.
3. **Cooper, S.** 1991. Bacterial growth and division. Biochemistry and regulation of prokaryotic and eukaryotic division cycles. Academic Press Inc., New York.
4. **Creanor, J., S. G. Elliott, Y. C. Bisset, and J. M. Mitchison.** 1983. Absence of step changes in activity of certain enzymes during the cell cycle of budding and fission yeasts in synchronous cultures. J. Cell Sci. **61**:339–349.
5. **de Koning, W., K. Groeneveld, L. J. W. M. Oehlen, J. A. Berden, and K. van Dam.** 1991. Changes in the activities of key enzymes of glycolysis during the cell cycle in yeast: a rectification. J. Gen. Microbiol. **137**:971–976.
6. **Gomes de Mesquita, D. S., R. ten Hoopen, and C. L. Woldringh.** 1991. Vacuolar segregation to the bud of *Saccharomyces cerevisiae*: an analysis of morphology and timing in the cell cycle. J. Gen. Microbiol. **137**:2447–2454.
7. **Gordon, C. N., and S. G. Elliott.** 1977. Fractionation of *Saccharomyces cerevisiae* cell populations by centrifugal elutriation. J. Bacteriol. **129**:97–100.
8. **Hartwell, L. H., and M. W. Unger.** 1977. Unequal division in *Saccharomyces cerevisiae* and its implications for the control of cell division. J. Cell Biol. **75**:422–435.
9. **Huls, P. G., N. Nanninga, E. A. van Spronsen, J. A. C. Valkenburg, N. O. E. Vischer, and C. L. Woldringh.** 1992. A computer-aided measuring system for the characterization of yeast populations combining 2D-image analysis, electronic particle counter, and flow cytometry. Biotechnol. Bioeng. **39**:343–350.
10. **Johnston, G. C., C. W. Ehrhardt, A. Lorincz, and B. L. A. Carter.** 1979. Regulation of cell size in the yeast *Saccharomyces cerevisiae*. J. Bacteriol. **137**:1–5.
11. **Kubitschek, H. E.** 1987. Buoyant density variation during the cell cycle in microorganisms. Crit. Rev. Microbiol. **14**:73–97.
12. **Lord, P. G., and A. E. Wheals.** 1980. Asymmetrical division of

Saccharomyces cerevisiae. J. Bacteriol. **142:**808–818.
13. **Lord, P. G., and A. E. Wheals.** 1983. Rate of cell cycle initiation of yeast cells when cell size is not a rate-determining factor. J. Cell Sci. **59:**183–201.
14. **Mitchison, J. M.** 1989. Cell cycle growth and periodicities, p. 205–237. *In* A. Nasim, P. Young, and B. F. Johnson (ed.), Molecular biology of the fission yeast. Academic Press Inc., New York.
15. **Oehlen, L. J. W. M., J. van Doorn, M. E. Scholte, P. W. Postma, and K. van Dam.** 1990. Changes in the incorporation of carbon derived from glucose into cellular pools during the cell cycle of *Saccharomyces cerevisiae*. J. Gen. Microbiol. **136:**413–418.
16. **Slater, M. L., S. O. Sharrow, and J. H. Gart.** 1977. Cell cycle of *Saccharomyces cerevisiae* in populations growing at different rates. Proc. Natl. Acad. Sci. USA **74:**3850–3854.
17. **Sudbery, P. E., and A. R. Goodey.** 1980. Genes which control cell proliferation in the yeast *Saccharomyces cerevisiae*. Nature (London) **288:**401–404.
18. **van Doorn, J., J. A. C. Valkenburg, M. E. Scholte, L. J. W. M. Oehlen, R. van Driel, P. W. Postma, N. Nanninga, and K. van Dam.** 1988. Changes in activities of several enzymes involved in carbohydrate metabolism during the cell cycle of *Saccharomyces cerevisiae*. J. Bacteriol. **170:**4808–4815.
19. **Vanoni, M., M. Vai, K. Popolo, and L. Alberghina.** 1983. Structural heterogeneity in populations of the budding yeast. J. Bacteriol. **156:**1282–1291.
20. **Wheals, A. E.** 1982. Size control models of *Saccharomyces cerevisiae* cell proliferation. Mol. Cell. Biol. **2:**361–368.